Regeneration of a model NO$_X$ storage/reduction catalyst using hydrocarbons as the reductant

Meshari AL-Harbi [a], David Radtke [b], William S. Epling [a,*]

[a] *Department of Chemical Engineering, University of Waterloo, Waterloo, Canada*
[b] *Department of Mechanical Engineering, Technical University of Braunschweig, Braunschweig, Germany*

ABSTRACT

Regeneration of a model NO$_X$ storage and reduction (NSR) catalyst using hydrocarbons, H$_2$, or CO as reducing agents was investigated. As previously shown, at low temperature, 200 °C, H$_2$ proved best, while both CO and hydrocarbons were found to poison Pt sites. At 250 °C, again H$_2$ was better but the decreased performance with CO and hydrocarbons was also due to slow kinetics and not solely as a result of Pt site poisoning. At $T \geq 300$ °C, hydrocarbons were found to regenerate the catalyst as efficiently as CO and H$_2$. Hydrocarbon steam reforming experiments were performed to investigate the improved performance at $T \geq 300$ °C. Steam reforming did not occur with either dodecane or m-xylene below 450 °C. Additionally, although propylene steam reforming occurred at 375 °C, the small amount of H$_2$ formed was insufficient for steam reforming to be the sole reason for improved regeneration. TPR experiments show that propylene was activated on the catalyst at $T \geq 217$ °C and, under the conditions examined, the complete reduction of NO by propylene was achieved at 287 °C. Furthermore, propylene was observed to reduce surface chemisorbed NO$_X$ species at $T > 200$ °C, with high rates by 264 °C, with this activity ultimately resulting in the comparable performance with either CO or H$_2$ at similar temperatures during NO$_X$ cycling experiments.

© 2010 Elsevier B.V. All rights reserved.

1. Introduction

With increasing environmental regulation pressure, reducing vehicle emissions has become a significant challenge facing automobile manufactures. This includes NO$_X$, CO and hydrocarbons, and there is increasing concern over vehicle CO$_2$ emissions as CO$_2$ is also considered a significant contributor to the greenhouse gas effect. One way to reduce vehicle CO$_2$ emissions and increase fuel economy is using lean-burn gasoline or diesel engines. However, lean-burn engine exhaust contains excess oxygen which makes NO$_X$ reduction challenging. One technology to reduce NO$_X$ emissions from lean-burn engines is NO$_X$ storage and reduction (NSR) catalysis. A NSR catalyst contains precious metals, such as Pt, Pd and Rh for the redox reactions, and alkali or alkaline metal earth components, such as Ba, that trap or store NO$_X$ as nitrite or nitrate species [1–4]. Overall, NO$_X$ is reduced to N$_2$ over NSR catalysts in five steps, two of which occur in the normal lean-burn exhaust environment, and the latter three in a reductant-rich mode, relative to oxygen [5–7]. These are called the lean and rich, or trapping and regeneration, phases of the cycle. The 5 steps are NO oxidation, NO$_2$ trapping, reductant evolution, nitrate decomposition and finally NO$_X$ reduc-

tion. In the lean phase, NO is oxidized to NO$_2$ and subsequently trapped by Ba in the form of a nitrate and/or nitrite. Upon saturation of some portion of the trapping material, the rich phase is required to regenerate the surface for further trapping capacity. In the rich phase, reductants, such as H$_2$, CO, and hydrocarbons (HCs), are introduced to induce nitrate/nitrite decomposition and reduce the trapped or released NO$_X$ to N$_2$.

Numerous approaches have been explored to achieve the net reducing environment in the rich phase to regenerate the catalyst and reduce the NO$_X$. These approaches include spraying diesel fuel into the exhaust (in-pipe injection) [8–10], using on-board fuel reformers to provide CO and H$_2$ [11,12], and in-cylinder injection of excess fuel (high F/A ratio) [13,14]. During this rich phase, it has been reported that diesel exhaust can, as an example, contain 2–6% CO, 1–2% H$_2$, 0.3–0.92% hydrocarbons and less than 0.5% O$_2$ [15–17]. In previous studies [17,18], different hydrocarbons species were detected in the diesel exhaust including formaldehyde, propylene, ethylene, acetylene, methane and dodecane. These hydrocarbons will be partially consumed by an upstream diesel oxidation catalyst (DOC) during the rich phase either via steam reforming or reacting with the small amount of oxygen in the gas or stored on the catalyst surface. However, some of these hydrocarbons will pass through the DOC to the downstream NSR catalyst. Researchers at Oak Ridge National Laboratory [18] have investigated the amount of reductant (CO, H$_2$, and HC) prior to and after the DOC and NSR

* Corresponding author. Tel.: +1 519 888 4567x37048.
  E-mail address: wepling@uwaterloo.ca (W.S. Epling).

catalysts, with the DOC placed upstream of the NSR catalyst. They found only a small change in reductant level across the DOC during the regeneration event, but a major decrease in the reductant levels across the NSR catalyst.

The hydrocarbons that pass through the DOC can be also be reformed during the rich phase over the NSR catalyst. Furthermore, several previous studies reported that the WGS reaction occurs on precious-metal based catalysts and on three way catalysts (TWCs) [19–23]. In one study, the WGS reaction over a commercial NSR catalyst [23] was investigated and the extent of the WGS reaction ranged from only 10% at 200 °C to 91% at 400 °C. This reductant amount change makes it difficult to determine whether the CO or H_2 is consistently the active reductant species. Previous work has demonstrated however, that isocyanate species form when CO is present, and these are hydrolyzed to form N_2 product [24,25]. This of course complicates the impact of CO, as it can react via the iso-cyanate route, or via the WGS reaction to form H_2. In terms of the hydrocarbon species, steam reforming can occur to produce H_2. Again, the H_2 produced can ultimately be used as the reductant source for NO_X reduction. The proposed likelihood of steam reform-ing over NSR catalysts is based on the ease of hydrocarbon steam reforming over precious metal based catalysts [26–31]. For exam-ple, previous studies have shown that steam reforming of CH_4, C_3H_8 and C_3H_6 begins at approximately 325 to 350 °C over Pd and Pt/Rh-based catalysts [30,31]. Such data indicate that if H_2 is a necessary reductant, then NSR catalyst regeneration using such hydrocarbon species may be limited at temperatures below ~350 °C, which is in the range that some authors have seen equivalent performance between HCs and H_2.

Regeneration of NSR catalysts using different reductants, such as H_2, CO, and hydrocarbons, and mixtures of these reductants, at dif-ferent operating temperatures has been investigated [7,32–42]. At low temperatures, there is a consensus that H_2 is better in compar-ison to CO and HC, possibly due to precious metal site poisoning [39,40] or Ba site poisoning by residual isocyanates [37,41]. At higher temperatures ($T \geq 300$ °C), H_2, CO, and HC are to some extent comparable in their regeneration and reduction efficiencies [40,42], therefore leaving the active reductant, whether it is H_2 or CO or hydrocarbon, ambiguous.

Although NSR regeneration phenomena have been investigated, to the best of our knowledge, the effects of HCs as the reducing agent on performance and trends in performance have not been systematically studied. In the present study, the regeneration of a NSR catalyst using representative HCs, propylene for short chain, dodecane for long chain and m-xylene for cyclic species, was eval-uated. Hydrogen and CO were also used for comparison with the HCs. Hydrocarbon steam reforming and temperature programmed reduction (TPR) experiments were also performed to characterize the performance changes observed as a function of temperature.

2. Experimental methods

A model $Pt/BaO/Al_2O_3$ monolith-supported sample, supplied by Johnson Matthey, was used in this study. The sample is composed of 2.0 g/in^3 Al_2O_3, 1.45% Pt and 20% BaO relative to the Al_2O_3. Via H_2 chemisorption, the Pt dispersion was found to be 12%. The sample had a cell density of 300 cpsi and was 2.1 cm in diameter and 6 cm in length. The catalyst was wrapped with 3 M catalytic converter matting material and inserted into a horizontal quartz tube reac-tor, which was placed inside a Lindberg temperature-controlled furnace. Two K-type thermocouples were placed at the radial cen-ter of the catalyst. One was just inside the inlet face of the catalyst and one just inside the outlet face of the catalyst. A third was placed approximately 1 in. upstream of the sample. Small quartz tubes, 3 mm OD and 2 mm ID, were placed upstream of the catalyst to

Table 1
Details of flow conditions used in the cycling experiments.

Flow conditions	Trapping (lean) phase	Regeneration (rich) phase
Space velocity	30,000 h^{-1}	30,000 h^{-1}
Concentrations		
NO	350 ppm	0
O_2	10%	0
CO_2	5%	5%
H_2O	5%	5%
H_2	0	1%
CO	0	1%
Hydrocarbons	0	1% relative to C1
N_2	Balance	Balance
Temperature (°C)		
170	40 s	10 s
200	40 s	5, 10, 20 s
250	60 s	5, 10, 20 s
300	80 s	10 s
350	100 s	10 s
400	120 s	10 s
500	80 s	10 s

prevent fully developed flow patterns and to assist in heat transfer from the furnace to the gas phase. Preliminary experiments with just an inert phase demonstrated that the temperature difference between the front and back of the catalyst was less than 5 °C for all flowrates and temperatures studied.

The gases and gas mixtures were supplied by Praxair. Bronkhorst mass flow controllers were used to meter the gases. For NSR cycling tests, a four-way, fast-acting solenoid valve was used to switch between the lean and rich mixtures, which were made in separate manifolds. Water was introduced downstream of this valve after the dry gas mixture had been heated. In experiments using dode-cane and xylene, the HCs were again metered with Bronkhorst mass flow controllers and introduced after the wet gas mixture had been heated to >170 °C to avoid condensation, and at the reactor inlet to avoid reactions on the steel tubing upstream of the quartz tube.

To start each cycling experiment with a consistent surface, before each experiment, the sample temperature was ramped to 500 °C and then cleaned, or conditioned, with a gas mixture con-sisting of 5% H_2O, 5% CO_2, 1% H_2, and a balance of N_2 for 15 min. The reactor was then cooled to the target test temperature. Cycling experiments were performed at 170, 200, 250, 300, 400 and 500 °C. Table 1 lists the gas compositions used in the cycling experiments. The gas compositions were measured using a MKS MultiGas 2030 FT-IR analyzer at approximately a 2 Hz collection rate. CO, CO_2, NO, NO_2, N_2O, NH_3, H_2O, C_3H_6, C_8H_{10}, and $C_{12}H_{26}$ concentrations were measured. In steam reforming experiments, spatially resolved capillary-inlet mass spectrometry (SpaciMS) was also used. The gases measured by the mass spectrometer were H_2, H_2O, C_3H_6, C_8H_{10}, $C_{12}H_{26}$ and Ar. Ar was used as a tracer in the mass spec-trometer for calibration purposes. Spatial resolution was achieved by placing a silica capillary, connected to the sampling end of a 6′ capillary from a Hiden Analytical mass spectrometer via a zero dead volume steel union fitting, within one of the radially centered catalyst channels. The capillary dimensions were 0.3 mm I.D. and 0.43 mm O.D. Gases were collected at different positions by moving the silica capillary tip to different positions within the channel.

Two types of TPR experiments were performed; one evaluating the reaction chemistry when C_3H_6 and NO were both introduced together in the gas phase, and one a surface reaction experiment where NO_X species were formed on the catalyst surface and C_3H_6 input after. In the former experiments, the catalyst was cleaned under the conditions described above and then cooled to 109 °C. The catalyst was then heated from 109 °C to 500 °C at a rate of about 3 °C/min in a mixture containing 1017 ppm C_3H_6, 257 ppm NO, 5% H_2O, and a N_2 balance. In the latter experiment, the catalyst was
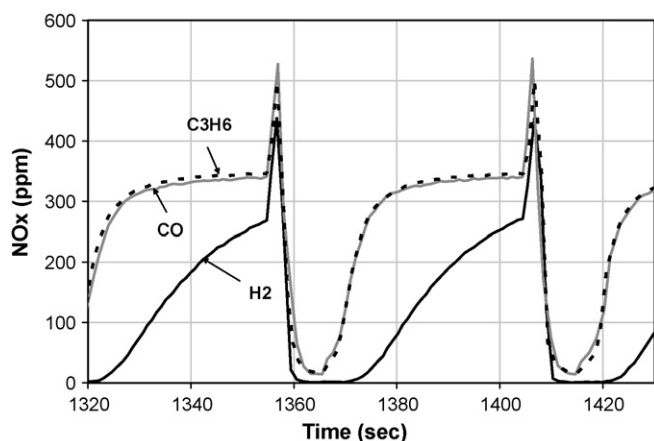
Fig. 1. NO_X outlet concentrations obtained at 170 °C with 1% H_2, 1% CO, or 3333 ppm C_3H_6.

heated to 300 °C and saturated with NO_X using a mixture containing 350 ppm NO, 10% O_2, 5% CO_2, 5% H_2O, and balance N_2. Then the reactor was cooled to 115 °C. The sample was then heated at about 2 °C/min to 500 °C in a mixture containing 55 ppm C_3H_6 and a N_2 balance. The products from the TPR experiments were monitored using the MKS MultiGas 2030 FT-IR analyzer.

3. Results and discussion

3.1. NO_X cycling experiments

Catalyst NO_X trapping and reduction performance results using different reductants at different temperatures are characterized in this section. This includes evaluating different HCs at the different temperatures to determine when they become efficient as reductants in the regeneration phase. The data shown in Fig. 1 were obtained at 170 °C. The lean, or trapping, time was 40 s and the rich, or regeneration, time was 10 s. The amounts of reductants

used were 1% H_2, 1% CO, or 0.33% C_3H_6 (1% on a C1 basis). Although the amount of C_3H_6 is greater than that of the CO or H_2 on a total reductant basis (in terms of the amount of O species that can be consumed via inclusion of H_2 and CO), an equivalent C1 basis was chosen for these experiments. The conversions and amounts of NO_X (the sum of NO and NO_2) trapped and released during these experiments are listed in Table 2. All reported values and plotted data were obtained after steady cycle-to-cycle performance was attained. The data shown in the figure and table demonstrate that H_2 resulted in better trapping performance, consistent with previous work [33,40,43]. Furthermore, at the onset of the lean phase, the outlet NO_X value reached 0 ppm for many seconds when H_2 was used, but not with CO and C_3H_6. With CO and C_3H_6, saturation of the available trapping sites occurred during the lean phase, whereas with H_2, the outlet NO_X level was still increasing at the end of the lean phase, not having reached the inlet value. The calculated NO_X conversions were 55, 7 and 6%, respectively, with differences primarily due to the significantly lower amounts trapped when using CO and C_3H_6. The total inlet NO_X during the 40-s lean time was 118 μmol. With H_2 and CO, 841 μmol were introduced during each regeneration period. Although fewer C_3H_6 moles were input, more was entered based on a C and H basis. The catalyst used in these experiments does not contain any oxygen storage components, such as ceria, so these reductant levels were in large excess relative to the amount required for complete reduction even if all the NO_X was trapped. Therefore, it is inactivity of the CO and C_3H_6 toward regeneration, thus leaving the catalyst surface covered with nitrates, which caused their poorer performance.

Experiments were carried out at higher temperatures to further investigate the effect of temperature on the storage, release, and reduction of NO_X with the different reductants. The outlet NO_X concentrations as a function of time at 250 °C are shown in Fig. 2. Dodecane and m-xylene were also tested as reductants at this temperature, again with 1% on a C1 basis as their inlet concentrations. The summary of the results is also listed in Table 2. For this set of experiments, the trapping time was 60 s and the regeneration time was 10 s. With CO, C_3H_6, C_8H_{10}, and $C_{12}H_{26}$, the NO_X breakthrough profiles during the lean phase were comparable. It should be men-

Table 2
Calculated performance characteristics as a function of temperature and reducing agent type. The calculated errors associated with these measurements were less than 1% for trapping conditions and less than 2% for regeneration conditions.

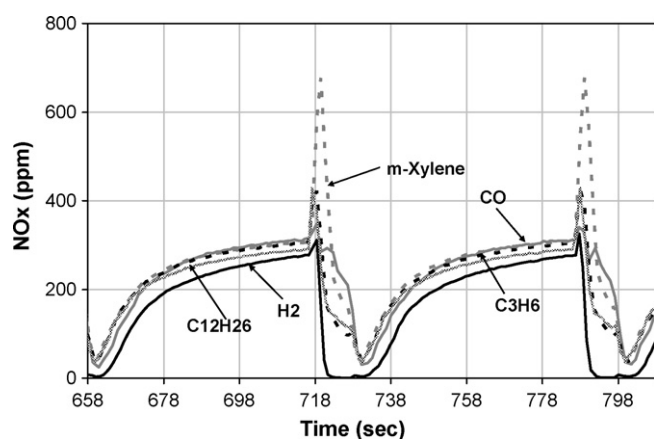| Temperature (°C)	Reductant	Time (s)		NO_X trapped (μmol)	NO_X released (μmol)	NO_X conversion (%)
		Lean	Rich			
170	H_2	40	10	74	9.4	55
	CO	40	10	23	14	7.2
	C_3H_6	40	10	21	13	6.4
250	H_2	60	10	81	7.3	42
	CO	60	10	56	25	18
	C_3H_6	60	10	60	24	20
	C_8H_{10}	60	10	52	27	14
	$C_{12}H_{26}$	60	10	63	18	25
300	H_2	80	10	156	6.4	64
	CO	80	10	140	10	55
	C_3H_6	80	10	135	14	51
	C_8H_{10}	80	10	114	33	34
	$C_{12}H_{26}$	80	10	135	15	51
400	H_2	120	10	259	24	67
	CO	120	10	237	31	58
	C_3H_6	120	10	270	16	72
	C_8H_{10}	120	10	250	17	66
	$C_{12}H_{26}$	120	10	251	15	67
500	H_2	80	10	115	38	32
	CO	80	10	117	55	26
	C_3H_6	80	10	118	31	37
	C_8H_{10}	80	10	100	22	33
	$C_{12}H_{26}$	80	10	101	21	34

Fig. 2. NO$_X$ outlet concentrations obtained at 250 °C with 1% H$_2$, 1% CO, 3333 ppm C$_3$H$_6$, 833 ppm C$_{12}$H$_{26}$, or 1250 ppm C$_8$H$_{10}$.

Fig. 3. NO$_X$ outlet concentrations obtained at 200 °C with different regeneration times; 5, 10, and 20 s. (A) 3333 ppm C$_3$H$_6$ and (B) 1% CO.

tioned that the catalyst performance improved, with CO and C$_3$H$_6$, compared to the performance observed at 170 °C. It is apparent that both hydrocarbons and CO have some activity toward regenerating the catalyst, albeit significantly less than the H$_2$. For H$_2$, the NO$_X$ conversion was actually less than that observed at 170 °C. This can occur for two reasons. One is simply the longer lean time at 250 °C, which will lead to lesser performance. Secondly, a similar trend has been noted before, where performance at temperatures as low as 100 °C were as high as those at 200, 250 and 300 °C. This trend was related to enhanced regeneration with H$_2$ when there are substantial hydroxyl amounts on the support surface and their promotion of reductant spillover to the trapping sites [44].

To decouple the effect of poisoning and slow kinetics, a second set of cycling experiments was performed, at 200 and 250 °C, where the rich-phase time was varied. The data obtained from experiments with CO and C$_3$H$_6$ at 200 °C are shown in Fig. 3. The lean phase was again 40 s but the regeneration times were 5, 10, and 20 s. No differences in trapping performance were observed when the regeneration time was increased from 5 to 20 s, using either reductant. Data obtained at 250 °C are shown in Table 3 and Fig. 4. The lean phase was 60 s and again the rich-phase duration was changed between 5, 10, and 20 s, with CO, C$_3$H$_6$, as well H$_2$. With all three reductants, increasing rich time resulted in increased performance, for example with CO, the amount trapped increased from 37 to 78 μmol with the increase from 5 to 20 s in rich time. The results shown in Fig. 4 also suggest that if the rich time was prolonged further, further regeneration might still occur.

The data obtained at 200 °C indicate that it is not simply slow kinetics during the rich phase limiting the extent of regeneration, since increasing the rich-phase time had no effect. It is also not a lack of reductant activation as some regeneration does occur, nor is it diffusional resistance differences between the reductants
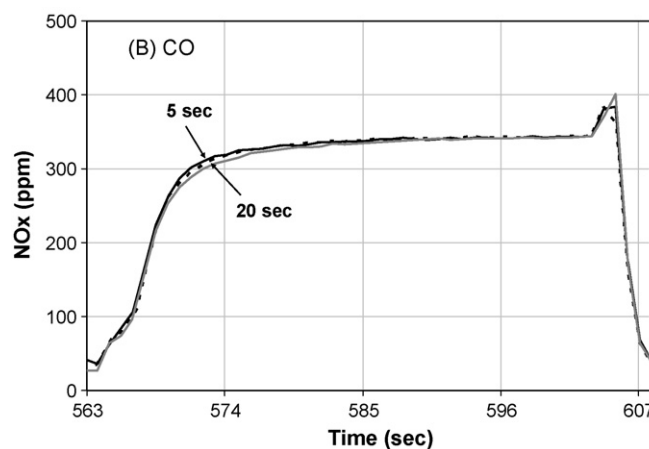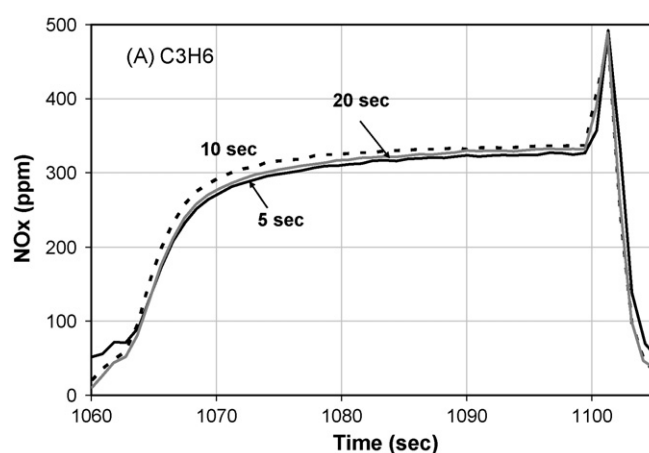
as increased time had no effect for the CO and C$_3$H$_6$ species. The poor performance is due to Pt site poisoning by CO and C$_3$H$_6$, thereby inhibiting the release and reduction reactions. This is in line with previous NSR catalyst studies using CO and C$_3$H$_6$ at low temperature. Abdulhamid et al. [40] investigated the regeneration of a Pt/BaO/Al$_2$O$_3$ catalyst using CO at 150, 250, and 350 °C and attributed the decrease in performance at low temperature to CO poisoning the Pt sites. In another study [45], surface IR results showed adsorbed CO and carbonate species when using CO or C$_3$H$_6$ at 200 °C as reductants, which also resulted in a lower NO$_X$ storage rate after the switch from the rich phase to the lean phase. However, the results at 250 °C indicate that the performance is limited by slow kinetics, although still possibly in combination with some residual Pt site poisoning. If poisoning was stronger/dominant, the

Table 3
Calculated performance characteristics as a function of reductant type and regeneration time at 250 °C.

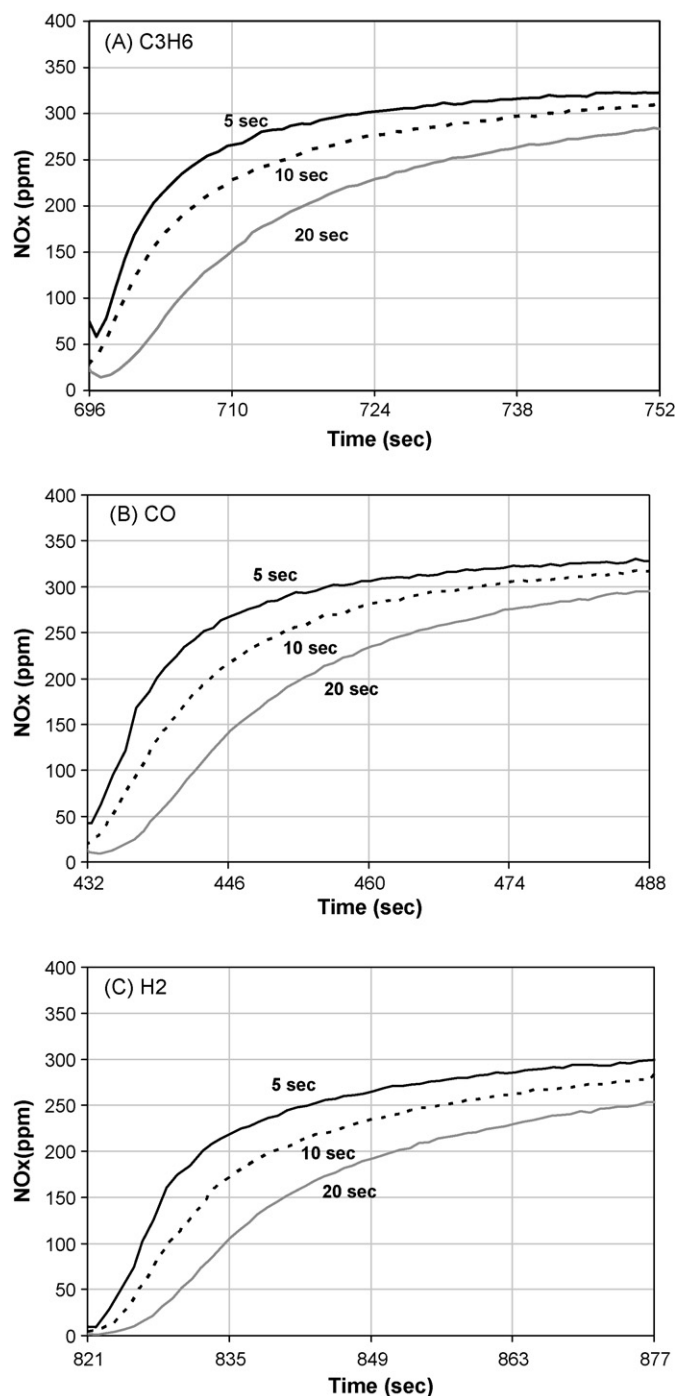| Reductant type	Time (s)		NO$_X$ trapped (μmol)	NO$_X$ released (μmol)	NO$_X$ conversion (%)
	Rich	Lean			
CO	5	60	37	15	13
	10	60	54	22	18
	20	60	78	31	27
C$_3$H$_6$	5	60	37	15	13
	10	60	55	17	21
	20	60	80	19	34
H$_2$	5	60	63	8	31
	10	60	81	6.8	42
	20	60	98	6	52

Fig. 4. NO_X outlet concentrations obtained at 250 °C with regeneration times; 5, 10, and 20 sec. (A) 3333 ppm C_3H_6, (B) 1% CO and (C) 1% H_2.

Fig. 5. NO_X outlet concentrations obtained at 300 °C with 1% H_2, 1% CO, 3333 ppm C_3H_6, 833 ppm $C_{12}H_{26}$, or 1250 ppm C_8H_{10}.

performance would not have improved with each increase in the rich time, as was the case at 200 °C. Surface diffusion limitations may play a role, but this would be coupled with poisoning. Previous work has shown isocyanate formation when CO was used as a reductant [41] and the authors concluded that these formed around the Pt sites, which could cause blocking of further surface transport. Such results also demonstrate that reductant spillover from the precious metal sites to the Ba trapping sites occurs, suggesting spillover direction.

The data obtained at 300 °C are shown in Fig. 5, with summary data listed in Table 2. There was an improvement in the catalyst performance with CO and hydrocarbons, relative to 250 °C, but H_2
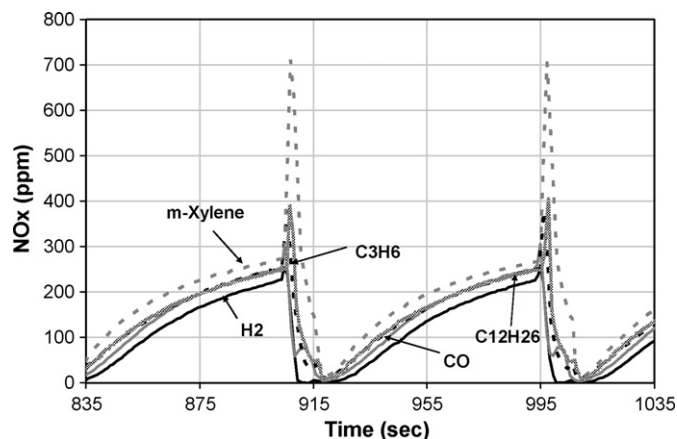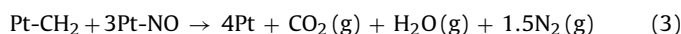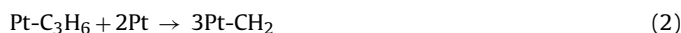
still showed better activity in both trapping and reduction performance. With H_2, the calculated NO_X conversion was 64%, while with CO it was 55%. Propylene and $C_{12}H_{26}$ led to slightly lower but similar conversions, indicating persistent kinetic limitations related to regeneration and reduction. With C_8H_{10}, the catalyst performance was significantly poorer, with the measured conversion being 34%. The poor performance with C_8H_{10} compared to C_3H_6 or $C_{12}H_{26}$ is likely related to its cyclic nature, where it is assumed that activation of cyclic hydrocarbons is more difficult than the straight chain hydrocarbons [46].

At 300 °C, NO_X trapping and conversion performance was better with H_2 compared to CO and hydrocarbons and CO was better than the hydrocarbons. The reasons for the improved performance with CO as the temperature was increased has been previously studied and is explained by decreased CO poisoning and increased hydrolysis of cyanates, which form from direct reduction of the nitrate species by CO [39,47]. In general, the increased performance at 300 °C when using the hydrocarbon reductants has been attributed to reductant activation vs. temperature [40]. Thus, as the temperature increased from 170 to 300 °C, the activation of hydrocarbons on the Pt sites became easier and faster, and poisoning effects decreased, resulting in the higher reduction activity. This is in line with previous work that has shown similar trends and concluded that once C–H bond activation occurred, HCs could act as reductants [48]. In terms of improved performance for all the reductants, there is an increased surface diffusion rate with temperature [6,49,50], higher NO oxidation rates [51,52], and higher nitrate/nitrite decomposition rates during regeneration [5,52], all of which typically lead to improved NSR catalyst performance at test temperatures below 400 °C.

Experiments at 400 and 500 °C were also performed with summary data listed in Table 2. At 400 °C, the amount of NO_X released was actually higher with H_2 relative to m-xylene and dodecane, leading to overall similar conversions. With C_3H_6, the catalyst performance was better than that observed with the other reductants, due to the higher overall reductant level introduced when counting both the H and C components as reductants. Similarly, there is more when using the m-xylene and dodecane, and with their similar performance to H_2, this suggests that there is still some limitation with their use. At 500 °C, catalyst performance was lower than that observed at 300, 350, and 400 °C, with all reductants. The amounts of NO_X trapped with H_2, CO and C_3H_6 were comparable, but there were differences in the amounts of NO_X released, with CO leading to higher release. Although the trapping performance was lower with C_8H_{10} and $C_{12}H_{26}$ compared to that observed with H_2, CO, and C_3H_6, the lower NO_X release during the rich phase led

to comparable conversions. The reason for the decreased performance relative to 300 and 400 °C is due to nitrate stability. The nitrate species decompose rapidly at the onset of regeneration due to their low thermal stability at high operating temperatures [53,54]. As the reductant is being used to regenerate NO_X species trapped at the upstream sites, NO_X species are rapidly decomposing at downstream sites and will travel through the catalyst without being reduced, leading to a lower ratio of rate of reduction to rate of NO_X release [55,56]. Also, due to their lower stability at higher temperature, less nitrates form during the trapping phase as well.

Two mechanisms have been proposed for reduction of NO_X to N_2 by hydrocarbons over the precious metal sites of NSR catalysts. The first mechanism [57] postulates that the reductant reduces the precious metal site, which then participates in NO decomposition. In the second mechanism [58], the reductant, C_3H_6 was selected as an example, is first adsorbed on the precious metal site and then breaks down to various types of reactive hydrocarbon subspecies [5]. The reactions pathways listed in reference [58] are shown below:

$$C_3H_6(g) + Pt \rightarrow Pt\text{-}C_3H_6 \tag{1}$$

$$Pt\text{-}C_3H_6 + 2Pt \rightarrow 3Pt\text{-}CH_2 \tag{2}$$

$$Pt\text{-}CH_2 + 3Pt\text{-}NO \rightarrow 4Pt + CO_2(g) + H_2O(g) + 1.5N_2(g) \tag{3}$$

For the sake of simplicity, the authors suggested CH_2 as the hydrocarbon sub-species formed from propylene decomposition. They proposed that the bound intermediate CH_2 group reacts with the sorbed NO_X species to form the reduction reaction products. In several IR characterization studies [48,59–62] nitro, organic nitro, nitrite and isocyanate surface species were observed on Ce-ZSM-5 and Pt/SiO_2 surfaces during lean-NO_X reduction tests and were suggested intermediates in this reaction process, supporting the CH_2-based mechanism shown above. However, a third possibility, due to the reaction mixtures imposed, is that hydrocarbons undergo steam reforming, producing CO and H_2, which act as the actual reductant species. This is discussed in the following section.

3.2. Hydrocarbon steam reforming

In cycling experiments, decreased catalyst performance at low temperatures using CO or hydrocarbons was related to Pt site poisoning, or slow kinetics as the temperature increased to 250 °C. However, at higher operating temperatures ($T \geq 300$ °C), there was a significant improvement in the catalyst performance using hydrocarbons. A similar improvement was observed with CO as the reductant as well, which has been well explained in recent literature [39,47], thus the focus of this discussion will be on the hydrocarbons. In the rich phase, hydrocarbons and H_2O are both present and therefore steam reforming could occur, leading to H_2 which could then act as the reductant. To investigate this possibility, hydrocarbon steam reforming was evaluated at different temperatures.

In this series of experiments, steam reforming of C_3H_6, $C_{12}H_{16}$, and C_8H_{10}, and mixtures of these, were investigated. The reaction gas mixtures used in these experiments contain 5% H_2O, 1% hydrocarbon on a C1 basis, and a balance of N_2. Experiments were carried out at different test temperatures, ranging between 250 and 525 °C with no reaction observed at less than 375 °C. Spatially resolved capillary-inlet mass spectrometry (SpaciMS) was used to quantify the amount of hydrocarbons, CO_2, H_2O, and H_2 at different catalyst positions. The capillary tip was moved to seven different positions within the channel to study the axial distribution of the species. In the plotted data, the zero position represents the inlet of sample and 6 cm is the end of sample.

Propylene steam reforming results, obtained along the catalyst length at different temperatures, are shown in Fig. 6. At 375 °C,
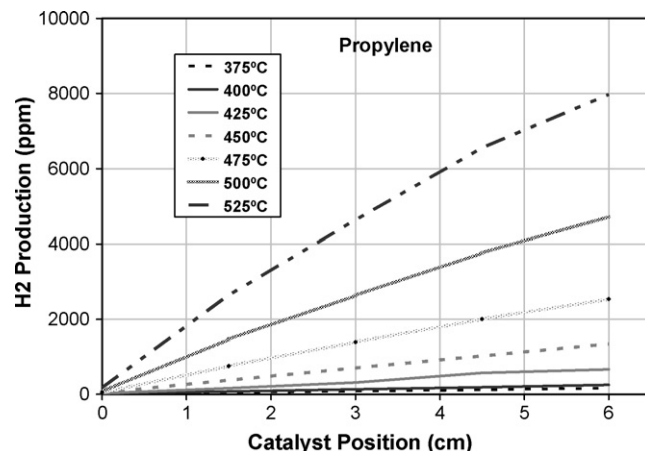

Fig. 6. H_2 concentrations obtained at different temperatures and lengths of the catalyst during steam reforming experiments. The inlet gas composition was 3333 ppm C_3H_6, 5% H_2O, and balance N_2.

C_3H_6 steam reforming occurs, but with very low conversions. As the temperature was increased to 525 °C, H_2 production monotonically increased, with more significant increases after 475 °C. H_2 production steadily increased as a function of catalyst length.

Similar experiments were also carried out, but with dodecane or m-xylene as the hydrocarbons. The H_2 production data as a function of temperature and axial length of the catalyst are shown in Figs. 7 and 8. Dodecane steam reforming started slightly below 450 °C, higher than that observed with C_3H_6 (375 °C). At 525 °C, H_2 production was 91, 690, and 1195 ppm at 0, 3, and 6 cm respectively, while the amount of H_2 formed with C_3H_6 at 525 °C was 172, 6551 and 7973 ppm. The outlet level with C_3H_6 was approximately 6.6 times higher than that observed with dodecane at the same temperature. m-Xylene steam reforming started at just below 475 °C and the amounts of H_2 formed were significantly lower than those with the other hydrocarbons. Again, H_2 formation increased with temperature, but even at 525 °C, only 20, 238, and 507 ppm were formed at 0, 3, and 6 cm inside of the sample, respectively, much lower than those observed with C_3H_6 and $C_{12}H_{26}$. These results, as expected, show that different hydrocarbon types undergo steam reforming at different temperatures and with different rates on the NSR catalyst. It should be noted that there is some measured conversion at the front of the catalyst at higher temperatures. The capillary tip is positioned at the very edge
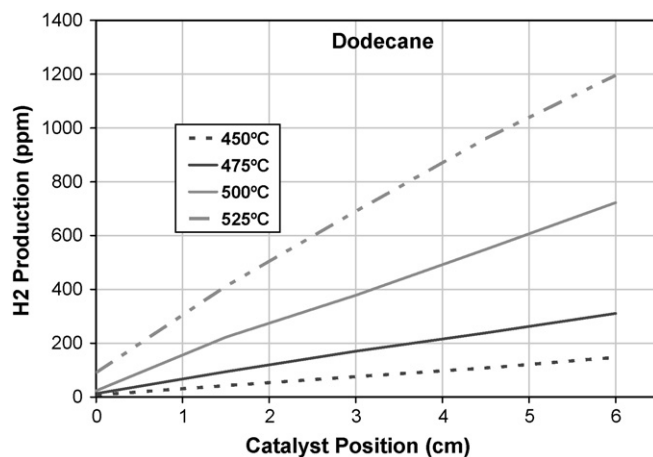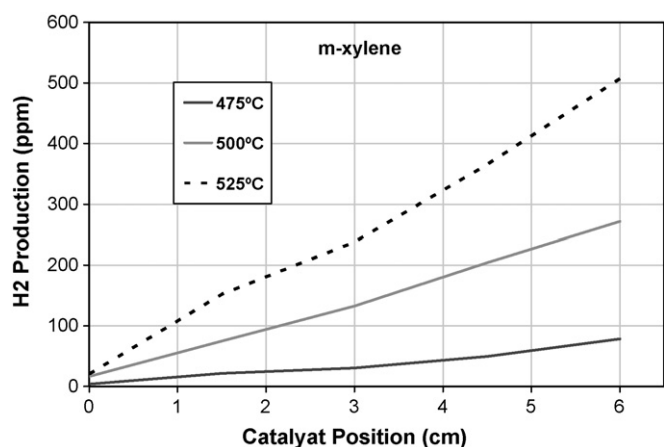

Fig. 7. H_2 concentrations obtained at different temperatures and lengths of the catalyst during steam reforming experiments. The inlet gas composition was 833 ppm $C_{12}H_{26}$, 5% H_2O, and balance N_2.

Fig. 8. H_2 concentrations obtained at different temperatures and lengths of the catalyst during steam reforming experiments. The inlet gas composition was 1250 ppm C_8H_{10}, 5% H_2O, and balance N_2.

Fig. 10. NO and C_3H_6 outlet concentrations obtained during a temperature programmed reduction experiment; the ramp rate was 3.3 °C/min. The inlet gas composition was 1017 ppm C_3H_6, 257 ppm NO, 5% H_2O, and balance N_2.

of the sample, so will probe conversion that could occur at the face. Also, dodecane and m-xylene will homogeneously decompose in the reactor at temperatures above 320–330 °C (based on empty reactor baseline experiments) and thus could lead to byproducts that are more easily reformed to H_2, even at or on the catalyst face.

H_2 production rates via steam reforming with a mixture of C_3H_6 and $C_{12}H_{26}$ were also investigated, with the data shown in Fig. 9. According to the results obtained, there was no change in the amount of dodecane in any of these tests demonstrating that no dodecane steam reforming occurred. C_3H_6 steadily decreased along the catalyst length; therefore, the amount of H_2 measured originated solely as a result of C_3H_6 steam reforming. There were only slight differences in the amount of H_2 formed via C_3H_6 steam reforming in the absence and presence of dodecane at both 375 and 400 °C. However, at the higher temperatures, significantly less H_2 was formed in the presence of dodecane. For example, at 525 °C and in the absence of dodecane, the amount of H_2 formed was 7973 ppm whereas in presence of dodecane, the amount of H_2 produced was 3738 ppm. This indicates that dodecane inhibited C_3H_6 steam reforming, but at the same time C_3H_6 inhibited dodecane steam reforming. The latter is likely due to the higher reactivity of the C_3H_6 while the former is possibly due to the coverage of some metallic sites by the longer chain hydrocarbons, resulting in lower availability of metallic sites for adsorption of reactants.
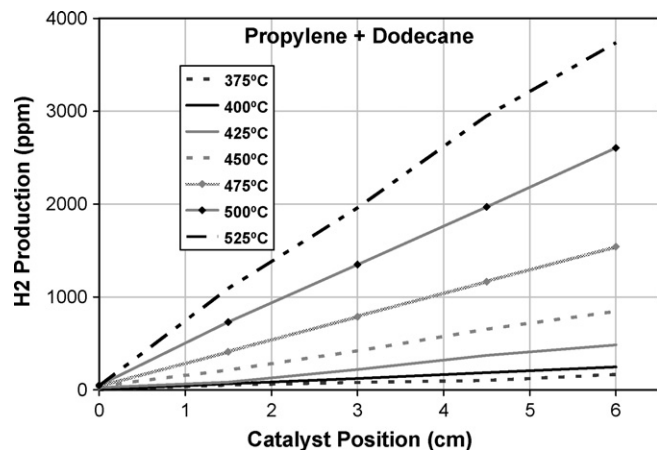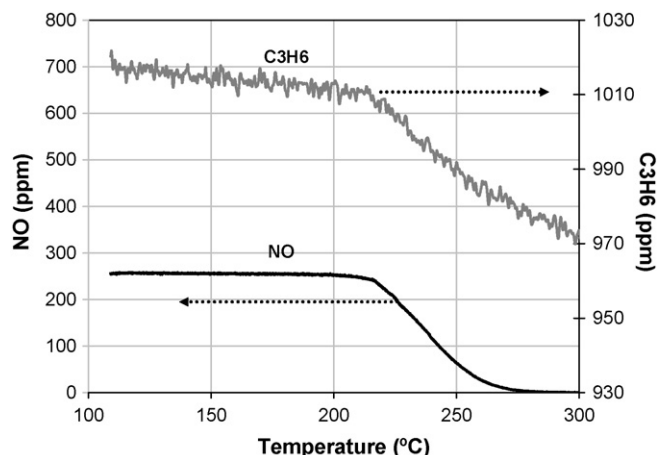
These results show that steam reforming over a NSR catalyst can occur when hydrocarbons and water are present in the gas stream. Different hydrocarbon types have different reactivities towards steam reforming. This could be related the extent of which the hydrocarbons can be activated on the surface of precious metals. Since steam reforming did not occur below 375 °C for C_3H_6 and 450 °C for $C_{12}H_{26}$ and C_8H_{10}, steam reforming cannot explain the improved performance in the cycling experiments at 300–400 °C described above. Furthermore, even at 375 and 450 °C, the amounts of H_2 produced were quite small, and built through the catalyst, such that at the catalyst front little H_2 was present until the higher temperatures. These data therefore demonstrate that steam reforming does not play a critical role in NSR regeneration below 450 °C. This is not to say that reforming is unimportant for NSR activity in general, as desulfation occurs at much higher temperatures, where steam reforming can have a more significant contribution.

3.3. TPR experiments

In the previous section, hydrocarbon steam reforming was investigated and the data show that reforming to H_2 is not significant enough to explain the improved performance observed above 300 °C when using hydrocarbons as reductants. To further investigate this issue, TPR experiments were performed with propylene selected as the reductant. Two types of experiments were performed; one where both the NO and C_3H_6 were simultaneously present in the gas phase and one where NO was first trapped on the catalyst and then C_3H_6 was input for the TPR.

In the first set of experiments, the catalyst was first cleaned with a gas mixture consisting of 5% H_2O, 5% CO_2, 1% H_2, and a balance of N_2 for 15 min at 500 °C. The reactor was then cooled to down to 109 °C. The catalyst was heated from 109 °C to 500 °C at approximately 3.3 °C/min in a mixture containing 1017 ppm C_3H_6, 257 ppm NO, 5% H_2O, and a N_2 balance. The profiles of C_3H_6 and NO consumption as a function of temperature are shown in Fig. 10. The reaction between C_3H_6 and NO started at approximately 200 °C, but at low rates and lit-off beginning at 217 °C. Full conversion of NO was observed by 287 °C. In terms of a mass balance, if the reduction equation is assumed as follows, $9NO + C_3H_6 \rightarrow 4.5N_2 + 3CO_2 + 3H_2O$, then for 9 moles of NO, 1 mole of C_3H_6 is required for reduction to N_2. At 287 °C, all inlet NO, 257 ppm, was consumed and therefore ~29 ppm of C_3H_6 should be consumed as well for the reduction. But, as shown in Fig. 10, approximately 41 ppm of C_3H_6 was consumed at 287 °C. The excess amount of C_3H_6 reacted went toward produc-
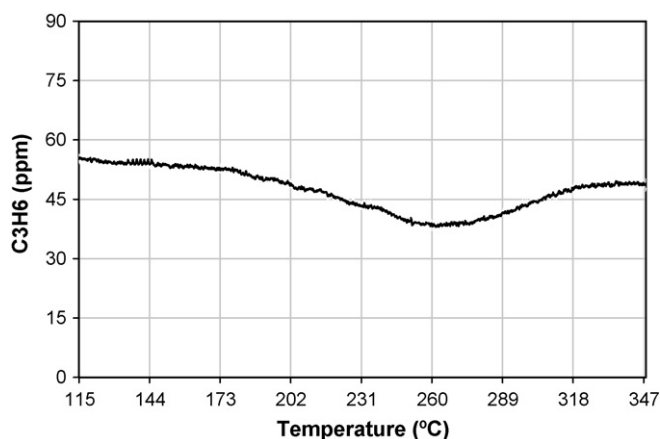

Fig. 9. H_2 concentrations obtained at different temperatures and lengths of the catalyst during steam reforming experiments. The inlet gas composition was 3333 ppm C_3H_6, 833 ppm $C_{12}H_{26}$, 5% H_2O, and balance N_2.

Fig. 11. C_3H_6 outlet concentrations obtained during a temperature programmed reduction experiment; the ramp rate was 2.1 °C/min. The catalyst was first heated to 300 °C and saturated with NO_X using a mixture containing 350 ppm NO, 10% O_2, 5% CO_2, 5% H_2O, and a N_2 balance. The reactor was then cooled to 115 °C to start the TPR experiment. The TPR gas composition contained 55 ppm C_3H_6 and a N_2 balance.

tion of CO and other short chain hydrocarbons via partial oxidation and reaction, as both CO and ethylene were detected by FT-IR. There have of course been several studies focused on NO_X reduction by hydrocarbons, but in the presence of O_2 (HC-SCR) [63–65]. Results from each of these studies indicate a similar temperature range in which C_3H_6 begins to reduce NO_X, even in the presence of O_2, again suggesting the activation of C_3H_6, or the HC species in general, as a determining factor for regeneration temperature dependency. Furthermore, and as discussed earlier, with a Pt/Ba/Al$_2$O$_3$ catalyst [37], a mixture containing C_3H_6 and O_2 reacted with surface NO_X species at approximately 230 °C, again in the same range as that observed here.

In the second experiment, the catalyst was heated to 300 °C and saturated with NO_X using a mixture containing 350 ppm NO, 10% O_2, 5% CO_2, 5% H_2O, and a N_2 balance. Then the reactor was cooled to 115 °C. The sample was then heated at 2.1 °C/min to 500 °C in a mixture containing 55 ppm C_3H_6 and a N_2 balance. Propylene consumption as a function of temperature is shown in Fig. 11. Little to no change in the C_3H_6 concentration was observed before 175 °C. Beyond that, there was a steady decrease in the C_3H_6 concentration until 264 °C, where the maximum consumption of C_3H_6 was observed. The C_3H_6 consumption rate then decreased beyond 272 °C as the surface NO_X species, thus reaction reactant, were depleted. Anderson et al performed TPR experiments on a Pt/Ba/Al$_2$O$_3$ catalyst with a stoichiometric C_3H_6/air mixture and observed maxima in NO_X release just above 200 °C [66]. This being done in an air-containing mixture resulted in some temperature increase due to the exotherm that would evolve from C_3H_6 combustion, thus their measured temperatures for NO_X release would be lower than those observed in our study. Furthermore, NO_X was not observed as a product with just C_3H_6 entering, indicating more complete reduction of the surface species. Jozsa et al. [33] also carried out TPR experiments, but on a commercial NSR catalyst, with C_3H_6, H_2, and CO. When the C_3H_6/N_2 mixture was used, NO_X release reached a plateau at 250 °C, slightly lower than that observed in our experiments. This is likely attributed to the trapping conditions, where NO_2 was stored between 60 and 100 °C. Saturating the catalyst at 300 °C, as in our study, would lead to states with higher stability than those formed with exposure at lower temperatures.

At 200 °C, as shown in Fig. 2, C_3H_6 and CO poisoning of Pt sites was evident by the lack of improvement with increased regeneration times. The TPR data in Fig. 10 show that NO reduction with C_3H_6 begins at temperatures slightly above 200 °C, with little activity at 200 °C, in-line with the cycling experiment data. At $T \geq 217$ °C,

the C_3H_6 and NO reaction is evident over the catalyst with complete reduction observed at 287 °C. Similarly, when reducing the previously trapped NO_X species (Fig. 11), some reaction extent is observed $\sim$200 °C, with increasing reactivity as the temperature was increased. Thus at 250 °C (Fig. 4), where extending the regeneration time did have a positive effect, it is related to slower kinetics, not complete poisoning by, or inactivity, of the hydrocarbon, nor to steam reforming of the hydrocarbon species. At $T \geq 287$ °C, based on the TPR and cycling experiments, the activation of C_3H_6 is not an issue and therefore a more comparable performance with H_2 would be expected.

4. Conclusions

In this study, the effects of different reducing agents (hydrocarbons, CO and H_2) on the performance of a model NSR catalyst were investigated. In cycling experiments, H_2 was the best reductant for catalyst regeneration at 170 °C and the poor performance with hydrocarbons and CO was due to Pt site poisoning. At 250 °C, H_2 was still superior and the poorer catalyst performance with hydrocarbons and CO was due to their slow reactivity and not solely because of poisoning effects. At $T \geq 300$ °C, hydrocarbons and CO were comparable with H_2. Hydrocarbon steam reforming experiment results show that steam reforming alone cannot explain the improved performance since steam reforming of dodecane and m-xylene occurred at $T \geq 450$ °C. With propylene, steam reforming occurred at 375 °C, but the small amount of H_2 formed was not enough to result in comparable performance to CO and H_2 in regenerating the NSR catalyst. TPR experiments were also performed and the results show that the reduction of NO by C_3H_6 can start at 217 °C. Moreover, propylene can also induce nitrate decomposition and reduction at $\sim$200 °C. Thus as the reaction temperature exceeds 200 °C, the hydrocarbons become directly active over the NSR catalyst, but are kinetically limited. At $T > 300$ °C, the regeneration-phase reaction rates with hydrocarbons become appreciable enough to make the extent of regeneration comparable to that with H_2.

References

[1] N. Takahashi, H. Shinjoh, T. Iijima, T. Suzuki, K. Yamazaki, K. Yokota, H. Suzuki, N. Miyoshi, S. Matsumoto, T. Tanizawa, T. Tanaka, S. Tateishi, K. Kasahara, Catalysis Today 27 (1996) 63.
[2] W. Bogner, M. Kramer, B. Krutzsch, S. Pischinger, D. Voigtlander, G. Wenninger, F. Wirbeleit, M. Brogan, R. Brisley, D. Webster, Applied Catalysis B: Environmental 7 (1995) 153.
[3] S. Matsumoto, Catalysis Today 29 (1996) 43.
[4] N. Miyoshi, S. Matsumoto, K. Katoh, T. Tanaka, J. Harada, N. Takahashi, K. Yokota, M. Sugiura, K. Kasahara, SAE Technical Paper 950809, 1995.
[5] W.S. Epling, L.E. Campbell, A. Yezerets, N.W. Currier, J.E. Parks, Catalysis Reviews 46 (2004) 163.
[6] B. Westerberg, E. Fridell, Journal of Molecular Catalysis A: Chemical 165 (2001) 249.
[7] S. Poulston, R.R. Rajaram, Catalysis Today 81 (2003) 603.
[8] J.E. Parks, A. Watson, G.C. Campbell, W.S. Epling, SAE Technical Paper Series 2002-01-2880.
[9] J.H. Stang, D.E. Koeberlein, M.J. Ruth, SAE Technical Paper Series 2001-01-2065.
[10] Y. Takahashi, Y. Takeda, N. Kondo, M. Murata, SAE Technical Paper Series 2004-01-0580.
[11] Y. Kong, S. Crane, P. Patel, B. Taylor, SAE Technical Paper Series 2004-01-0582.
[12] N. Khadiya, S. Crane, C. Huffmeyer, B. Taylor, SAE Technical Paper Series 2004-01-2648.
[13] D. Tomazic, M.M. Tatur, M.J. Thornton, SAE Technical Paper Series 2004-01-0581.
[14] K. Nakatani, S. Hirota, S. Takeshima, K. Itoh, T. Tanaka, SAE Technical Paper Series 2002-01-0957.

[15] S. Huff, B.H. West, J. Parks, M. Swartz, J. Green, R. Graves, SAE Technical Paper Series 2006-01-1416.
[16] H. Mahzoul, P. Gilot, J.-F. Brilhac, B.R. Stanmore, Topics in Catalysis 16/17 (2001) 293.
[17] M. Swartz, S. Huff, J. Parks, B.H. West, SAE Technical Paper Series 2006-01-3423.
[18] B.H. West, S. Huff, J. Parks, S. Lewis, J.-S. Choi, W. Partridge, J. Storey, SAE Technical Paper Series 2004-01-3023.
[19] C. Serre, F. Garin, G. Belot, G. Marie, Journal of Catalysis 141 (1993) 1.
[20] J. Barbier, D. Duprez, Applied Catalysis B: Environmental 3 (1993) 61.
[21] J. Kaspar, P. Fornasiero, N. Hickey, Catalysis Today 77 (2003) 419.
[22] J. Botas, M. Gutierrez-Ortiz, M. Gonzalez-Marcos, J. Gonzalez-Marcos, J. Gonzalez-Velasco, Applied Catalysis B: Environmental 32 (2001) 243.
[23] M. AL-Harbi, W.S. Epling, A. Yezerets, N.W. Currier, H.-Y Chen, H. Hess, SAE Technical Paper Series 2009-01-0631.
[24] T. Szailer, J.H. Kwak, D.H. Kim, J.C. Hanson, C.H.F. Peden, J. Szanyi, Journal of Catalysis 239 (2006) 51.
[25] J.P. Breen, R. Burch, C. Fontaine-Gautrelet, C. Hardacre, C. Rioche, Applied Catalysis B: Environmental 81 (2008) 150.
[26] T. Maillet, C. Solleau, J. Barbier, D. Duprez, Applied Catalysis B: Environmental 14 (1997) 85.
[27] A. Donazzi, A. Beretta, G. Groppi, P. Forzatti, Journal of Catalysis 255 (2008) 241.
[28] S. Lima, I. Cruz, G. Jacobs, B.H. Davis, L.V. Mattos, F.B. Noronha, Journal of Catalysis 257 (2008) 356.
[29] X. Wang, R.J. Gorte, J.P. Wagner, Journal of Catalysis 212 (2002) 225.
[30] F. Arosio, S. Colussi, A. Trovarelli, G. Groppi, Applied Catalysis B: Environmental 80 (2008) 335.
[31] J. Barbier, D. Duprez, Applied Catalysis A: General 85 (1992) 89.
[32] M. Konsolakis, I.V. Yentekakis, Applied Catalysis B: Environmental 29 (2001) 103.
[33] P. Jozsa, E. Jobson, M. Larsson, Topics in Catalysis 30–31 (2004) 177.
[34] D. James, E. Fourreï, M. Ishii, M. Bowker, Applied Catalysis B: Environmental 45 (2003) 147.
[35] T. Lesage, C. Verrier, P. Bazin, J. Saussey, M. Daturi, Physical Chemistry Chemical Physics 5 (2003) 4435.
[36] Z. Liu, J.A. Anderson, Journal of Catalysis 224 (2004) 18.
[37] C.M.L. Scholz, B.H.W. Maes, M.H.J.M. de Croon, J.C. Schouten, Applied Catalysis A: General 332 (2007) 1.
[38] C.M.L. Scholz, K.M. Nauta, M.H.J.M. de Croon, J.C. Schouten, Chemical Engineering Science 63 (2008) 2843.
[39] M. AL-Harbi, W.S. Epling, Applied Catalysis B: Environmental 89 (2009) 315.
[40] H. Abdulhamid, E. Fridell, M. Skoglundh, Topics in Catalysis 30/31 (2004) 161.
[41] I. Nova, L. Lietti, P. Forzatti, F. Frola, F. Prinetto, G. Ghiotti, Topics in Catalysis 52 (2009) 1757.
[42] C. Narula, S. Nakouzi, R. Wu, C. Goralski, L. Allard, Journal of AIChE 47 (2001) 744.
[43] Jae-Soon Choi*, William P. Partridge, C. Stuart Daw, Applied Catalysis A: General 293 (2005) 24.
[44] L. Lietti, I. Nova, P. Forzatti, Journal of Catalysis 257 (2008) 270.
[45] P.-H. Han, Y.-K. Lee, S.-M. Han, H.-K. Rhee, Topics in Catalysis 16/17 (2001) 165.
[46] R. Burch, P.J. Millington, Catalysis Today 26 (1995) 185.
[47] W. Epling, J. Parks, N. Currier, A. Yezerets, Catalysis Today 96 (2004) 21.
[48] Y. Li, S. Roth, J. Dettling, T. Buetel, Topics in Catalysis 16–17 (2001) 139.
[49] L. Liotta, G. Pantaleo, A. Macaluso, G. DiCarlo, G. Deganello, Applied Catalysis A: General 245 (2003) 167.
[50] J. Despres, M. Elsener, M. Koebel, O. Krocher, B. Schnyder, A. Wokaun, Applied Catalysis B: Environmental 50 (2004) 73.
[51] L. Olsson, B. Westerberg, H. Persson, E. Fridell, M. Skoglundh, B. Andersson, Journal of Physical Chemistry B 103 (1999) 10433.
[52] J.M. Coronado, J.A. Anderson, Journal of Molecular Catalysis A: Chemical 138 (1999) 83.
[53] W.S. Epling, A. Yezerets, N.W. Currier, Catalysis Letters 110 (2006) 143.
[54] E. Fridell, M. Skoglundh, B. Westerberg, S. Johansson, G. Smedler, Journal of Catalysis 183 (1999) 196.
[55] E. Fridell, H. Persson, B. Westerberg, L. Olsson, M. Skoglundh, Catalysis Letters 66 (2000) 71.
[56] A. Obuchi, A. Ohi, M. Nakamura, A. Ogata, K. Mizuno, H. Ohuchi, Applied Catalysis B: Environmental 2 (1993) 71.
[57] R. Burch, J. Breen, F. Meunier, Applied Catalysis B: Environmental 39 (2002) 283.
[58] L. Olsson, E. Fridell, M. Skoglundh, B. Andersson, Catalysis Today 73 (2002) 263.
[59] C. Yokoyama, M. Misono, Journal of Catalysis 150 (1994) 9.
[60] H. Hamada, Y. Kintaichi, M. Inaba, M. Tabata, T. Yoshinari, H. Tsuchida, Catalysis Today 29 (1996) 53.
[61] T. Okuhara, Y. Hasada, M. Misono, Catalysis Today 35 (1997) 83.
[62] T. Maunula, J. Ahola, H. Hamada, Applied Catalysis B: Environmental 26 (2000) 173.
[63] J.M. García-Cortés, J. Pérez-Ramírez, M.J. Illán-Gómez, F. Kapteijn, J.A. Moulijn, C. Lecea, Applied Catalysis B: Environmental 30 (2001) 399.
[64] E. Joubert, X. Courtois, P. Marecot, D. Duprez, Applied Catalysis B: Environmental 64 (2006) 103.
[65] R. Burch, D. Ottery, Applied Catalysis B: Environmental 13 (1997) 105.
[66] J.A. Anderson, B. Bachiller-Baezaa, M. Fernández-García, Physical Chemistry Chemical Physics 5 (2003) 4418.